

Volume polarization holographic recording in thick photopolymer for optical memory

Shiuan Hwei Lin,^{1*} Sheng-Lung Cho,² Shin-Fu Chou,¹ June Hua Lin,⁴ Chih Min Lin,² Sien Chi^{3,4} and Ken Yuh Hsu⁴

¹Department of Electrophysics, National Chiao Tung University, HsinChu 30010, Taiwan

²Department of Electrical Engineering, Yuan Ze University, Chungli, 32003, Taiwan

³Department of Photonics Engineering, Yuan Ze University, Chungli, 32003, Taiwan

⁴Department of photonics & Institute of Electro-Optical Engineering, National Chiao Tung University, HsinChu 30010, Taiwan

*lin@cc.nctu.edu.tw

Abstract: Based on a vector wave theory of volume holograms, dependence of holographic reconstruction on the polarization states of the writing and reading beams is discussed. It is found that under paraxial approximation the circular polarization holograms provide a better distinction of the reading beams. Characteristics of recording polarization holograms in thick phenanthrenequinone-doped poly(methyl methacrylate) (PQ/PMMA) photopolymer are experimentally investigated. It is found that the circular polarization holographic recording possesses better dynamic range and material sensitivity, and a uniform spatial frequency response over a wide range. The performance is comparable to that of the intensity holographic recording in PQ/PMMA. Based on theoretical analyses and the material properties, a polarization multiplexing holographic memory using circularly polarization recording configuration for increasing storage capacity has been designed and experimentally demonstrated.

©2014 Optical Society of America

OCIS codes: (210.2860) Holographic and volume memories; (090.0090) Holography; (090.2900) Optical storage materials.

References and links

1. G. Barbastathis and D. Psaltis, "Volume holographic multiplexing methods," in *Holographic data storage* (Springer, 2000), pp. 21–62.
2. T. Todorov, L. Nikolova, K. Stoyanova, and N. Tomova, "Polarization holography. 3: Some applications of polarization holographic recording," *Appl. Opt.* **24**(6), 785–788 (1985).
3. J. Eickmans, T. Bieringer, S. Kostromine, H. Berneth, and R. Thoma, "Photoaddressable polymers: a new class of materials for optical data storage and holographic memories," *Jpn. J. Appl. Phys.* **38**(3S), 1835–1836 (1999).
4. R. Hagen and T. Bieringer, "Photoaddressable polymers for optical data storage," *Adv. Mater.* **13**(23), 1805–1810 (2001).
5. L. L. Nedelchev, A. S. Matharu, S. Hvilsted, and P. S. Ramanujam, "Photoinduced anisotropy in a family of amorphous azobenzene polyesters for optical storage," *Appl. Opt.* **42**(29), 5918–5927 (2003).
6. H. Ono, T. Sekiguchi, A. Emoto, T. Shioda, and N. Kawatsuki, "Light wave propagation and Bragg diffraction in thick polarization gratings," *Jpn. J. Appl. Phys.* **47**(10 10R), 7963–7967 (2008).
7. L. Nikolova and P. S. Ramanujam, *Polarization holography* (Cambridge University, 2009).
8. K. Kawano, T. Ishii, J. Minabe, T. Niitsu, Y. Nishikata, and K. Baba, "Holographic recording and retrieval of polarized light by use of polyester containing cyanoazobenzene units in the side chain," *Opt. Lett.* **24**(18), 1269–1271 (1999).
9. W. D. Koek, N. Bhattacharya, J. J. Braat, V. S. Chan, and J. Westerweel, "Holographic simultaneous readout polarization multiplexing based on photoinduced anisotropy in bacteriorhodopsin," *Opt. Lett.* **29**(1), 101–103 (2004).
10. H. Wei, L. Cao, Z. Xu, Q. He, G. Jin, and C. Gu, "Orthogonal polarization dual-channel holographic memory in cationic ring-opening photopolymer," *Opt. Express* **14**(12), 5135–5142 (2006).
11. S. Pu, B. Yao, G. Liu, and Y. Wang, "Polarization multiplexing holographic optical recording of a new photochromic diarylethene," *Opt. Eng.* **47**(3), 030502 (2008).
12. D. Barada, Y. Kawagoe, H. Sekiguchi, T. Fukuda, S. Kawata, and T. Yatagai, "Volume polarization holography for optical data storage," in *SPIE OPTO*, (International Society for Optics and Photonics, 2011), 79570Q.

13. D. Barada, T. Ochiai, T. Fukuda, S. Kawata, K. Kuroda, and T. Yatagai, "Dual-channel polarization holography: a technique for recording two complex amplitude components of a vector wave," *Opt. Lett.* **37**(21), 4528–4530 (2012).
14. P. Yeh, *Introduction to photorefractive nonlinear optics* (Wiley, 1993).
15. K. Kuroda, Y. Matsuhashi, R. Fujimura, and T. Shimura, "Theory of Polarization Holography," *Opt. Rev.* **18**(5), 374–382 (2011).
16. T. Huang and K. Wagner, "Coupled mode analysis of polarization volume hologram," *IEEE J. Quantum Electron.* **31**(2), 372–390 (1995).
17. L. Nikolova and T. Todorov, "Diffraction efficiency and selectivity of polarization holographic recording," *J. Mod. Opt.* **31**(5), 579–588 (1984).
18. K. Y. Hsu, S. H. Lin, Y. N. Hsiao, and W. T. Whang, "Experimental characterization of phenanthrenequinone-doped poly(methyl methacrylate) photopolymer for volume holographic storage," *Opt. Eng.* **42**(5), 1390–1396 (2003).
19. S. H. Lin, P. L. Chen, and J. H. Lin, "Phenanthrenequinone-doped copolymers for holographic data storage," *Opt. Eng.* **48**(3), 035802-1- 035802-7 (2009).
20. A. Trofimova, A. Stankevich, and V. Mogilnyi, "Phenanthrenequinone–polymethylmethacrylate composite for polarization phase recording," *J. Appl. Spectrosc.* **76**(4), 585–591 (2009).
21. C. I. Chuang, Y. N. Hsiao, S. H. Lin, and Y. F. Chao, "Real-time measurement of photo-induced effects in 9,10-phenanthrenequinone-doped poly(methyl methacrylate) photopolymer by phase-modulated ellipsometry," *Opt. Commun.* **283**(17), 3279–3283 (2010).
22. S. H. Lin, P. L. Chen, C. I. Chuang, Y. F. Chao, and K. Y. Hsu, "Volume polarization holographic recording in thick phenanthrenequinone-doped poly(methyl methacrylate) photopolymer," *Opt. Lett.* **36**(16), 3039–3041 (2011).

1. Introduction

Among the key techniques for holographic memory the holographic multiplexing schemes are the most important ones [1], because they allow us to efficiently make use of the huge capacity potential of volume storage. Conventional multiplexing schemes for volume holograms include angle-, wavelength-, phase-, shift- and peristrophic-multiplexing. Basically, these schemes are based on the Bragg condition in volume hologram provided by a thick medium. In addition to these conventional schemes, polarization multiplexing is another possibility, which makes use of the polarization state of light waves in a polarization-sensitive recording medium [2–7]. By combining the conventional holographic multiplexing and the polarization multiplexing in a polarization-sensitive medium the storage capacity can be potentially increased. Several experimental implementations named as dual-channel polarization-multiplexing holography have been demonstrated in previous works [8–13]. In their works, two data pages with orthogonal polarizations were recorded one by another on the same storage area using a reference beam with the same polarization. After recording, the two orthogonally polarized signals were reconstructed simultaneously by one reading beam. The two images were separated by a polarization beam splitter and imaged onto two CCDs. Thus, the storage capacity and the data rate of the system could be increased by two times.

Another possible scheme for polarization multiplexing is to record two data pages on the same area with the signal waves remain at a single polarization yet the two reference waves in orthogonal polarizations [7]. After recording, the two recorded data pages can be reconstructed independently onto one CCD device by a reading beam with the corresponding polarization state. Since only the polarization state of the reference and that of the reading beams need to be tuned for holograms recording and reconstruction, the architecture of this optical system is close to that of conventional holographic multiplexing systems. And therefore, this scheme would provide a convenient way for combining the holographic multiplexing and the polarization multiplexing techniques so as to increase the storage capacity. Nevertheless, in either scheme, in order to achieve a full utilization of polarization multiplexing volume holograms, it is necessary to understand the polarization characteristics of volume hologram. Further, it is necessary to know the holographic properties, such as recording sensitivity and diffraction efficiency, of different polarizations in such a polarization sensitive recording medium.

Thus, in this paper, we first present a vector wave theory of polarization volume holograms. Dependence of the reconstructed wave on the polarization states of the writing and reading beams will be described in detail. Then, in Section 3, we describe experimental studies on polarization holographic recording in a polarization sensitive holographic material, Phenanthrenequinone-doped Poly(methyl methacrylate) (PQ/PMMA) photopolymer. Holographic characteristics including recording dynamic range and material sensitivity of multiplexed polarization holograms will be presented. In Section 4, based on the theoretical analyses and the holographic characteristics of PQ/PMMA, we describe the design of a polarization multiplexing holographic memory. Optical experiments are demonstrated. Then, conclusions are given in Section 5.

2. Theoretical basis

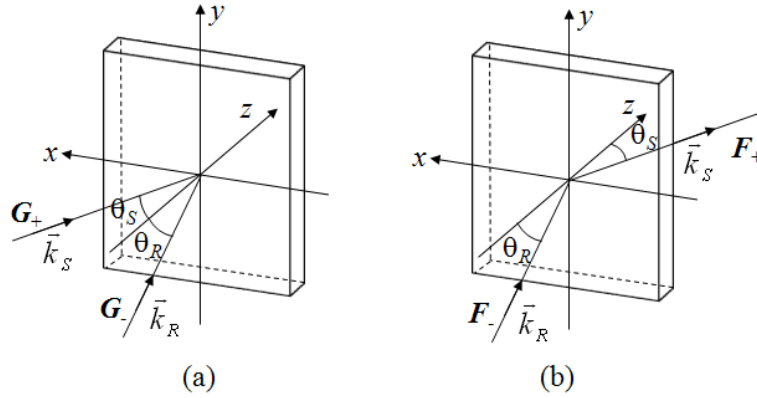


Fig. 1. Schematic diagram of holographic recording (a) and reconstruction (b).

Vector wave theory of volume holography can be found in previous works [14, 15]. Here, we summarize their results and will be focusing on the dependence of the holographic reconstruction on light polarizations. Figure 1 shows a typical schematic diagram for holographic recording and reconstruction. During the recording stage, shown in Fig. 1(a), we consider the signal wave, a plane wave with vector amplitude \vec{G}_+ incident at angle θ_S and the reference wave, a plane wave with vector amplitude \vec{G}_- incident at angle θ_R . The resultant electric field of the interference pattern can be written as

$$\vec{E} = \vec{G}_+ \exp(i\vec{k}_S \cdot \vec{r}) + \vec{G}_- \exp(i\vec{k}_R \cdot \vec{r}) \quad (1)$$

where \vec{k}_S and \vec{k}_R are the wave vectors of signal and reference waves, respectively, written as

$$\vec{k}_S = \begin{bmatrix} k \sin \theta_S \\ 0 \\ k \cos \theta_S \end{bmatrix}, \quad \vec{k}_R = \begin{bmatrix} k \sin \theta_R \\ 0 \\ k \cos \theta_R \end{bmatrix} \quad (2)$$

where k is the wave number of the recording beams. Note that in our coordinate system the angles θ_S and θ_R are with opposite signs, i.e., $\theta_S = -\theta_R$ for the symmetrical incidence. Then, during the hologram reconstruction stage, shown in Fig. 1(b), one would like to find the reconstructed wave \vec{F}_+ corresponding to the reading beam with vector amplitude \vec{F}_- .

Without loss of generality and for the purpose of investigating polarization dependence of the hologram reconstruction, here we assume the reading beam to be incident at the same angle θ_R of the reference beam such that the Bragg condition is satisfied. In addition, for mathematical simplicity, we choose the coordinate system to be associated with the s-polarized

and p-polarized beams of the reference and signal beams in Fig. 1, respectively, and the two unit vectors are defined as

$$\hat{s}_j = \begin{bmatrix} 0 \\ 1 \\ 0 \end{bmatrix}, \hat{p}_j = \begin{bmatrix} \cos \theta_j \\ 0 \\ -\sin \theta_j \end{bmatrix} \quad (3)$$

where \hat{s}_j and \hat{p}_j ($\varphi = P, \Sigma$) represent unit vectors of s-polarization and p-polarization, respectively. The suffixes “ Σ ” and “ P ” denote the signal and reference beams. In the following, we consider two kinds of holographic gratings according to the polarization states of the writing beams.

2.1 Index grating: two non-orthogonal writing beams

When the polarization states of two writing beams are non-orthogonal, the recorded hologram is called intensity hologram, because it is the intensity pattern of the optical interference that is recorded. When the intensity pattern is recorded in a phase medium such as photorefractive crystals and photopolymers, a refractive index variation followed on the intensity of the interference field is created such that the hologram is the index grating. This is the typical situation of a phase hologram recording. For this case, the refractive index variation of the medium can be represented by

$$n(\vec{r}) = n_0 + n_1 \cos \left[(\vec{k}_s - \vec{k}_r) \cdot \vec{r} \right] \quad (4)$$

where n_0 is uniform refractive index of the material, and n_1 is the amplitude of index modulation, given by,

$$n_1 \propto \mathbf{G}_+ \cdot \mathbf{G}_-^* \quad (5)$$

Equation (5) indicates that the refractive index hologram can be recorded only by the reference and signal beams with non-orthogonal polarization states.

By using the coupled wave theory for polarized waves [14] and assuming weak grating, the vector amplitude \mathbf{F}_+ of the reconstructed signal can be derived as

$$\mathbf{F}_+ \propto (\mathbf{G}_+ \cdot \mathbf{G}_-^*) \left[\mathbf{F}_- - (\mathbf{F}_- \cdot \hat{k}_s) \hat{k}_s \right] \quad (6)$$

where \hat{k}_s is unit wave vector of the reconstructed signal.

Now let us examine the influence of the polarization states of the writing and reading beams on holographic recording and reconstruction. Consider a particular case of holographic recording with left-handed circularly polarized waves, in which both the object and reference beams are left-handed circularly polarized. The vector amplitudes of the object, reference, and reading waves \mathbf{G}_+ , \mathbf{G}_- and \mathbf{F}_- , respectively, can be written as

$$\begin{aligned}
\mathbf{G}_+ &= G_+ \hat{L}_S = \frac{G_+}{\sqrt{2}} (\hat{s}_S + i\hat{p}_S) = \frac{G_+}{\sqrt{2}} \begin{bmatrix} i \cos \theta_S \\ 1 \\ -i \sin \theta_S \end{bmatrix}, \\
\mathbf{G}_- &= G_- \hat{L}_R = \frac{G_-}{\sqrt{2}} (\hat{s}_R + i\hat{p}_R) = \frac{G_-}{\sqrt{2}} \begin{bmatrix} i \cos \theta_R \\ 1 \\ -i \sin \theta_R \end{bmatrix} \\
\mathbf{F}_- &= F_- \hat{L}_R = \frac{G_-}{\sqrt{2}} (\hat{s}_R + i\hat{p}_R) = \frac{G_-}{\sqrt{2}} \begin{bmatrix} i \cos \theta_R \\ 1 \\ -i \sin \theta_R \end{bmatrix}
\end{aligned} \tag{7}$$

In the above equations, \hat{L}_j ($j = R, S$) represent unit vectors of left-handed circular polarization for the reference and the signal waves, respectively. By substituting Eq. (7) into Eq. (6), the vector amplitude \mathbf{F}_+ of the reconstructed signal can be obtained as

$$\mathbf{F}_+ \propto \frac{G_+ G_-^* F_- (1 - \cos(\theta_S - \theta_R))}{2\sqrt{2}} (\hat{s}_S + i \cos(\theta_S - \theta_R) \hat{p}_S) \tag{8}$$

Equation (8) indicates that, in general, the reconstructed signal \mathbf{F}_+ is elliptically polarized, and the circular polarization state of the original signal wave \mathbf{G}_+ is not correctly retrieved. It can also be seen that there is no cross term in the retrieval between the p-polarized and s-polarized components of the reading wave, i.e., the s-polarized component of the reconstructed signal is diffracted by the s-polarized component of the reading wave, and so is the p-polarized component. However, because the coupling constant of the p-polarized wave is different from that of the s-polarized wave, thus the polarization state of the reconstructed signal may not be the same as that of the original signal wave, unless the optical waves are linearly polarized. Note that right-handed circular polarization writing beams would bear similar characteristics as that of the left-handed polarization beams in the index grating, and linear polarization can be considered as a special case of circular polarization. Thus, above results can be extended to general index gratings which are recorded and retrieved by other polarization states.

2.2 Polarization grating: two orthogonal writing beams

When the polarization states of the writing beams are orthogonal, the holograms are called the polarization gratings. In this case, the intensity distribution of the interference field is uniform so that this type of hologram records the periodic polarization pattern that is generated by the summation of the signal and reference vector waves by using the photoinduced anisotropy of polarization-sensitive medium. When the polarization pattern is exposed in such a medium, a periodic birefringe variation followed on the polarization state of the interference field is created. By using the coupled wave theory of vector waves in [15] and assuming weak grating, the vector amplitude \mathbf{F}_+ of the reconstructed signal can be written as

$$\mathbf{F}_+ \propto \mathbf{X}_+ + \left\{ \mathbf{X}_- - (\mathbf{X}_- \cdot \hat{k}_S) \hat{k}_S \right\} \tag{9}$$

where vectors \mathbf{X}_+ and \mathbf{X}_- are represented by

$$\begin{aligned}
\mathbf{X}_+ &= B_1 (\mathbf{G}_-^* \cdot \mathbf{F}_-) \mathbf{G}_+ \\
\mathbf{X}_- &= A (\mathbf{G}_+ \cdot \mathbf{G}_-^*) \mathbf{F}_- + B_2 (\mathbf{G}_+ \cdot \mathbf{F}_-) \mathbf{G}_-^*
\end{aligned} \tag{10}$$

where A , B_1 and B_2 are constants given in Ref [15], which are functions of material properties and the recording configuration. It is seen in Eq. (10) that vector \mathbf{X}_+ is proportional to the original signal wave \mathbf{G}_+ . On the other hand, the polarization state of vector \mathbf{X}_- is not the same

as that of the signal wave \mathbf{G}_+ . Thus, the resultant polarization state of reconstructed signal \mathbf{F}_+ may not be the same as that of the original signal. In the following, we consider the situations of linearly and circularly polarized lights separately, because they are the most frequent cases for practical applications.

2.2.1 Orthogonal linear polarization

In this case, both the object and the reference beams are linearly polarized and the polarization states are orthogonal to each other. There are two possible combinations for the object \mathbf{G}_+ and the reference beams \mathbf{G}_- : Case 1(a), the s-polarized object and p-polarized reference waves; and Case 1(b), the p-polarized object and s-polarized reference waves. For Case 1(a), the vector amplitudes \mathbf{G}_+ and \mathbf{G}_- are written respectively as

$$\mathbf{G}_+ = G_+ \hat{s}_S = G_+ \begin{bmatrix} 0 \\ 1 \\ 0 \end{bmatrix}, \quad \mathbf{G}_- = G_- \hat{p}_R = G_- \begin{bmatrix} \cos \theta_R \\ 0 \\ -\sin \theta_R \end{bmatrix} \quad (11a)$$

For Case 1(b), the vector amplitudes \mathbf{G}_+ and \mathbf{G}_- are written respectively as

$$\mathbf{G}_+ = G_+ \hat{p}_S = G_+ \begin{bmatrix} \cos \theta_S \\ 0 \\ -\sin \theta_S \end{bmatrix}, \quad \mathbf{G}_- = G_- \hat{s}_R = G_- \begin{bmatrix} 0 \\ 1 \\ 0 \end{bmatrix} \quad (11b)$$

In order to investigate the dependence of the reconstructed signal on the polarization state of the reading beam, we consider two possible polarization states of the reading beam \mathbf{F}_- , s-polarization and p-polarization, which are written respectively as

$$\mathbf{F}_- = F_- \hat{s}_R = F_- \begin{bmatrix} 0 \\ 1 \\ 0 \end{bmatrix}, \quad \text{or} \quad \mathbf{F}_- = F_- \hat{p}_R = F_- \begin{bmatrix} \cos \theta_R \\ 0 \\ -\sin \theta_R \end{bmatrix} \quad (12)$$

By substituting Eqs. (11a), (11b) and (12) into Eqs. (9) and (10), we obtain the vector amplitude \mathbf{F}_+ of the reconstructed signal, which is summarized in Table 1. It can be seen in column \mathbf{F}_+ that the polarization state of the reconstructed signal is the same as that of the original signal \mathbf{G}_+ , if the polarization state of the reading beam \mathbf{F}_- is identical to that of the reference beam \mathbf{G}_- . However, the polarization of the reconstructed signal will be rotated by 90° if that of the reading beam is rotated by 90° . Therefore, there is always a diffracted wave reconstructed from the polarization hologram, and the polarization state will be either parallel or orthogonal to that of the object wave, depending on that of the reading wave.

Table 1. Vector Amplitude \mathbf{F}_+ Reconstructed from Orthogonal Linear Polarization Hologram by Different Polarization States

case	\mathbf{G}_+	\mathbf{G}_-	\mathbf{F}_-	\mathbf{F}_+
1(a)	$G_+ \hat{s}_S$	$G_- \hat{p}_R$	$F_- \hat{p}_R$	$B_1 G_-^* F_- G_+ \hat{s}_S$
			$F_- \hat{s}_R$	$B_2 G_-^* F_- G_+ \cos(\theta_S - \theta_R) \hat{p}_S$
1(b)	$G_+ \hat{p}_S$	$G_- \hat{s}_R$	$F_- \hat{s}_R$	$B_1 G_-^* F_- G_+ \hat{p}_S$
			$F_- \hat{p}_R$	$B_2 G_-^* F_- G_+ \cos(\theta_S - \theta_R) \hat{s}_S$

2.2.2 Orthogonal circular polarization

In this case, both the object and the reference waves are circularly polarized, and they are orthogonal to each other. Again, there are two possible combinations for the object \mathbf{G}_+ and the reference beams \mathbf{G}_- : Case 2(a), the left-handed circularly polarized object wave and

right-handed circularly polarized reference wave; and Case 2(b), the right-handed circularly polarized object wave and left-handed circularly polarized reference wave.

For Case 2(a), the vector amplitudes \mathbf{G}_+ and \mathbf{G}_- are written respectively as

$$\begin{aligned}\mathbf{G}_+ &= G_+ \hat{L}_S = \frac{G_+}{\sqrt{2}} (\hat{s}_S + i\hat{p}_S) = \frac{G_+}{\sqrt{2}} \begin{bmatrix} i \cos \theta_S \\ 1 \\ -i \sin \theta_S \end{bmatrix}, \\ \mathbf{G}_- &= G_- \hat{R}_R = \frac{G_-}{\sqrt{2}} (\hat{s}_R - i\hat{p}_R) = \frac{G_-}{\sqrt{2}} \begin{bmatrix} -i \cos \theta_R \\ 1 \\ i \sin \theta_R \end{bmatrix}\end{aligned}\quad (13a)$$

For Case 2(b), the vector amplitudes \mathbf{G}_+ and \mathbf{G}_- are written respectively as

$$\begin{aligned}\mathbf{G}_+ &= G_+ \hat{R}_S = \frac{G_+}{\sqrt{2}} (\hat{s}_S - i\hat{p}_S) = \frac{G_+}{\sqrt{2}} \begin{bmatrix} -i \cos \theta_S \\ 1 \\ i \sin \theta_S \end{bmatrix}, \\ \mathbf{G}_- &= G_- \hat{L}_R = \frac{G_-}{\sqrt{2}} (\hat{s}_R + i\hat{p}_R) = \frac{G_-}{\sqrt{2}} \begin{bmatrix} i \cos \theta_R \\ 1 \\ -i \sin \theta_R \end{bmatrix}\end{aligned}\quad (13b)$$

In the above equations, \hat{L}_j and \hat{R}_j ($j = R, S$) represent unit vectors of left-handed and right-handed circular polarization, respectively. After recording, the hologram can be reconstructed by a reading beam with either left-handed circular or right-handed circular polarization, of which the wave amplitude \mathbf{F} is written as

$$\begin{aligned}\mathbf{F}_- &= F_- \hat{L}_R = \frac{F_-}{\sqrt{2}} (\hat{s}_R + i\hat{p}_R) = \frac{F_-}{\sqrt{2}} \begin{bmatrix} i \cos \theta_R \\ 1 \\ -i \sin \theta_R \end{bmatrix}, \text{ or} \\ \mathbf{F}_- &= F_- \hat{R}_R = \frac{F_-}{\sqrt{2}} (\hat{s}_R - i\hat{p}_R) = \frac{F_-}{\sqrt{2}} \begin{bmatrix} -i \cos \theta_R \\ 1 \\ i \sin \theta_R \end{bmatrix}\end{aligned}\quad (14)$$

Similarly, by substituting Eqs. (13a), (13b), and (14) into Eqs. (9) and (10) the vector amplitude \mathbf{F}_+ of the reconstructed signal can be obtained. The results are summarized in Table 2. It can be seen in Table 2 that in general for all cases, the polarization state of the reconstructed wave are complicated and elliptically polarized. It is only when the polarization state of the reading beam is identical to that of the reference beam, plus under paraxial approximation, the original object wave can be exactly reconstructed. To satisfy paraxial approximation, the intersection angle between the reference and the object beams must be so small that they propagate almost along the axial direction. Then, $\theta_S \approx \theta_R \approx 0^\circ$, and the coefficient $\cos(\theta_S - \theta_R) \approx 1$. Under this condition, the polarization state of the diffracted signal becomes circular and is the same as that of the original signal. We also note that, under paraxial approximation and with the reading beam orthogonally polarized to that of the reference beam, no diffraction at all will occur from the polarization hologram. Therefore, holographic reconstructions with orthogonally polarized reading waves can achieve a very high degree of distinction for the two reading beams. Comparing this with that of orthogonal linear polarization hologram described in Cases (1a) and (1b), orthogonal circular polarization hologram is superior in terms of the signal to noise ratio for the reconstructed waves. These results are consistent with previous works derived by Huang and Wagner [16] and Nikolova et

al [17]. They assumed the paraxial approximation and used 2x2 Jones matrix method to derive the diffraction properties from a polarization grating.

These analyses provide solutions to design hybrid polarization and other Bragg-condition based multiplexing scheme for holographic data storage system. However, the performance of recording material to reproduce these theoretic analyses and to have enough dynamic range of refractive index change is also critical. Thus, in the following section, we present experimental studies on the characteristics of volume polarization holograms which are recorded in our photopolymer material PQ/PMMA. Then, the hybrid polarization and peristrophic multiplexing holographic data storage system using PQ/PMMA is proposed and demonstrated.

Table 2. Vector Amplitude F_+ Reconstructed from Orthogonal Circular Polarization Hologram by Different Polarization States

case	G_+	G_-	F_-	F_+	
				non-paraxial approximation	paraxial approximation
2(a)	$G_+ \hat{L}_S$	$G_- \hat{R}_R$	$F_- \hat{R}_R$	$G_-^* F_- G_+ B_1 \hat{L}_S + G_-^* F_- G_+ \left[\begin{array}{l} \frac{A}{2\sqrt{2}} (1 - \cos(\theta_S - \theta_R)) \cdot (\hat{s}_S - i \cos(\theta_S - \theta_R) \hat{p}_S) \\ \frac{B_2}{2\sqrt{2}} (1 + \cos(\theta_S - \theta_R)) \cdot (\hat{s}_S + i \cos(\theta_S - \theta_R) \hat{p}_S) \end{array} \right]$	$\left[G_-^* F_- G_+ B_1 + \frac{B_2}{\sqrt{2}} G_-^* F_- \right]$
			$F_- \hat{L}_R$	$G_-^* F_- G_+ \left[\frac{A+B_2}{2\sqrt{2}} \right] \cdot (1 - \cos(\theta_S - \theta_R)) \cdot (\hat{s}_S + i \cos(\theta_S - \theta_R) \hat{p}_S)$	0
2(b)	$G_+ \hat{R}_S$	$G_- \hat{L}_R$	$F_- \hat{L}_R$	$G_-^* F_- G_+ B_1 \hat{R}_S + G_-^* F_- G_+ \left[\begin{array}{l} \frac{A}{2\sqrt{2}} (1 - \cos(\theta_S - \theta_R)) \cdot (\hat{s}_S + i \cos(\theta_S - \theta_R) \hat{p}_S) \\ \frac{B_2}{2\sqrt{2}} (1 + \cos(\theta_S - \theta_R)) \cdot (\hat{s}_S - i \cos(\theta_S - \theta_R) \hat{p}_S) \end{array} \right]$	$\left[G_-^* F_- G_+ B_1 + \frac{B_2}{\sqrt{2}} G_-^* F_- \right]$
			$F_- \hat{R}_R$	$G_-^* F_- G_+ \left[\frac{A+B_2}{2\sqrt{2}} \right] \cdot (1 - \cos(\theta_S - \theta_R)) \cdot (\hat{s}_S - i \cos(\theta_S - \theta_R) \hat{p}_S)$	0

3 Characteristics of polarization holograms in PQ/PMMA photopolymer

The recording material used in this study is PQ/PMMA photopolymer fabricated in our laboratory. It consists of a host matrix PMMA doped with MMA monomer and photosensitive PQ molecules. The characteristics of multiplexed index holograms recorded in this material have been described in previous works [18, 19]. Holographic experiments using a 2-mm thick sample with an argon laser at wavelength 514 nm demonstrated that dynamic range, $M\#$ of 3.35 and holographic recording sensitivity, S of $0.6 \text{ cm}^2 \cdot \text{J}^{-1}$, and photo-induced shrinkage coefficient smaller than 10^{-5} have been achieved. Hundreds of volume gratings have been

successfully recorded and reconstructed at one position of this material. In order to achieve polarization multiplexing, the characteristics of polarization hologram recording in PQ/PMMA should be tested.

The photo-induced birefringence and the ability of volume polarization holographic recording in PQ/PMMA photopolymer have been demonstrated in previous studies [20–22]. Experimental results show that the diffraction efficiency of a polarization grating depends strongly on the total intensity of the recording beams. With the optimal intensity of $26 \text{ mW}\cdot\text{cm}^{-2}$, the maximal diffraction efficiency of the hologram can reach to $\sim 7\%$ for the orthogonal linear polarization recording configuration, and that can reach to $\sim 40\%$ for the orthogonal circular polarization recording configuration. Here, we used the same laser intensity for characterizing polarization holographic recording. A two-beam interference optical setup (shown as in Fig. 2) following the schematic diagram shown in Fig. 1 was conducted. A plane wave of argon laser at 514 nm was split into two beams with an intensity ratio at 1:1, and they were incident onto the PQ/PMMA sample symmetrically with an intersection angle of 2θ in air.

3.1 The dependence of the holographic reconstruction on light polarizations

Firstly, we examine the theoretic results in section 2. For probing the polarization state of the reconstructed signal, a polarizer mounted on a rotational stage was added on the arm of diffracted beam behind the PQ/PMMA sample. The power (P) of the diffracted beam from hologram was monitored by detector D1 when the transmission axis of the polarizer was rotated. It was plotted as a function of the azimuth angle (α) between the transmission axis and the incident plane by using a polar coordinate (P, α). Figures 2(b) and (c) show typical curves when the signal wave is set to be circularly or linearly polarized, respectively. It is seen that a dot circle indicates the polarization state of the light wave to be either left-handed or right-handed circular polarized. The shapes of “8” and “ ∞ ” indicate s-polarization and p-polarizations, respectively.

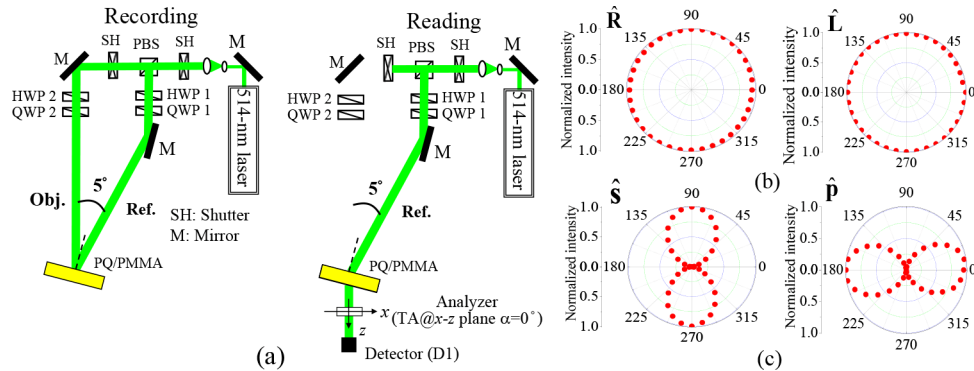


Fig. 2. (a) Optical setup for recording and reconstructing polarization hologram in PQ/PMMA and polar coordinate plot for signal beam with (b) circular polarization and (c) linear polarization.

To verify the theoretical analyses of the polarization dependence diffraction from either index grating or polarization grating in section 2, we have reconstructed holograms recorded by four different polarization configurations with $2\theta = 5^\circ$. The experimental results are summarized in the Tables 3 and 4. The second column in the table shows the polarization states of the signal beam G_+ and the reference beam G_- , respectively. The third and fourth columns show the plots of reconstructed signals under different the reading beam F . It is seen, in Table 3 that for the index grating recorded by either linear or circular polarization, the polarization of the reconstructed signal is the same as that of the reading beam. In contrast, for polarization grating the results are consistent to the case 2(a) under paraxial approximation in Table 2. When the hologram is recorded by orthogonal linear polarization in Table 4, there is always a

diffracted wave, and the polarization state of F_+ is orthogonal to that of the reading wave F_- . In addition, for polarization grating recorded with orthogonal circular polarization, a strong diffracted beam can be obtained if the polarization state of the reading beam F_- is identical to that of the reference beam G_- . The polarization state of the original object wave can be exactly reconstructed. However, with the reading beam orthogonally polarized to that of the reference beam, very weak diffraction is obtained from the hologram. This phenomenon demonstrates the high degree of distinction of holographic reconstructions for the two reading beams.

Table 3. Polarization States of the Diffracted Signals from the Intensity Hologram

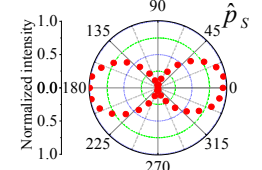
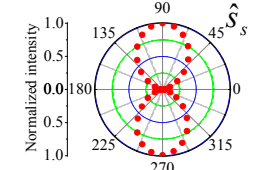
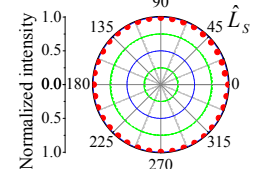
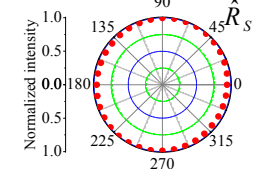
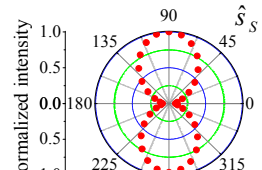
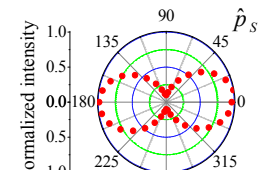
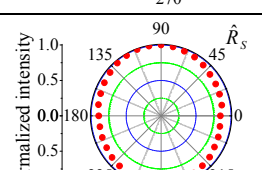
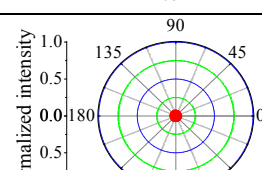
case	G_+	G_-	F_-	F_+	F_-	F_+
3(a)	$G_+ \hat{S}_S$	$G_- \hat{S}_R$	$F_- \hat{P}_R$		$F_- \hat{S}_R$	
3(b)	$G_+ \hat{L}_S$	$G_- \hat{L}_R$	$F_- \hat{L}_R$		$F_- \hat{R}_R$	

Table 4. Polarization States of the Diffracted Signals from a Polarization Hologram

case	G_+	G_-	F_-	F_+	F_-	F_+
4(a)	$G_+ \hat{P}_S$	$G_- \hat{S}_R$	$F_- \hat{P}_R$		$F_- \hat{S}_R$	
4(b)	$G_+ \hat{R}_S$	$G_- \hat{L}_R$	$F_- \hat{L}_R$		$F_- \hat{R}_R$	

3.2 Characteristics of multiple polarization holographic recording

Secondly, we characterize the performance of multiple polarization holographic recording in PQ/PMMA. The intersection angle of two recording beams was firstly set to be 30° in air at first. At one position of the photopolymer material, one set of 175 holograms of orthogonal linear polarizations was recorded by using the peristrophic multiplexing technique. During the recording of each hologram, the object beam was s-polarized and the reference beam p-polarized with respect to the grating vector, respectively. Then, the reference beam was used for the hologram reconstruction after each recording. Similarly, at another position, the second set of 175 polarization holograms was recorded. In this set, the polarization states of the two recording beams were right-handed circularly polarized and left-handed circularly polarized with respect to the grating vector, respectively.

In order to perform the peristrophic multiplexing the sample was mounted on a rotation stage with its rotation axis in parallel to the bisection of the two recording beams. The exposure

energy density for each hologram was $0.23 \text{ J}\cdot\text{cm}^{-2}$. The diffraction efficiency (defined as the ratio of the intensity of the diffracted beam to that of the summation of the diffracted and the transmitted beams) of each grating was measured after recording. The summation of the square roots of the diffraction efficiencies forms a running curve of the cumulative grating strength, i.e. $C(E) = \sum_{i=1}^n \sqrt{\eta_i}$, where n is the total number of holograms that have been recorded at the cumulative exposure energy E ($\text{J}\cdot\text{cm}^{-2}$). By curve fitting with the function: $C(E) = C_{\text{sat}}[1 - \exp[-(E/E_{\tau})]]$, the saturation value C_{sat} of the curve gives the dynamic range of the material, $M\#$ and E_{τ} gives the exposure energy constant of the material. The material sensitivity, S , is defined as an increment in the cumulative grating strength with respect to the energy of that exposure. When the sample is fresh or below chemically exhausted, $S = dC(E)/dE|_{E \rightarrow 0} = M\# / E_{\tau}$, according to the running curve function. Thus, holographic characteristics of the material can be obtained once the cumulative grating curve has been measured.

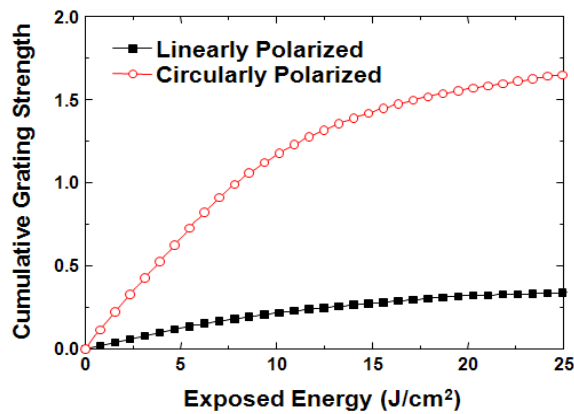


Fig. 3. The cumulative grating strengths for orthogonal circular and linear polarizations as a function of exposure energy in the PQ/PMMA sample.

The running curves of the cumulative grating strengths for the two sets of polarization holograms are shown in Fig. 3. From these curves $M\#$ and S of the material for each set of polarization holograms can be calculated, as summarized in Table 5. It can be seen that $M\#$ and S are strongly dependent on the polarization configuration during recording. The circularly polarized type possesses better holographic properties and the performance is comparable to that of the index hologram shown in Ref [18].

Table 5. $M\#$ and S for Different Recording Configurations with Orthogonally Polarized Writing Beams

Case	$M\#$	S ($\text{cm}^2\cdot\text{J}^{-1}$)
Linear polarization	0.43	0.03
Circular polarization	1.82	0.18

Further, we also investigated the dependence of $M\#$ and S on the recording angles 2θ under orthogonal circular polarization configuration. The running curves of the cumulative grating strength for different writing angles are shown in Fig. 4. The corresponding values of $M\#$ and S are calculated and summarized in Table 6. It can be seen that both $M\#$ and S remain almost constant for a big range of writing angles, which indicates that PQ/PMMA photopolymer provides a uniform spatial frequency response over a wide range. These experimental results are very useful for designing polarization multiplexing holographic memory in PQ/PMMA photopolymer material, as will be described in the following section.

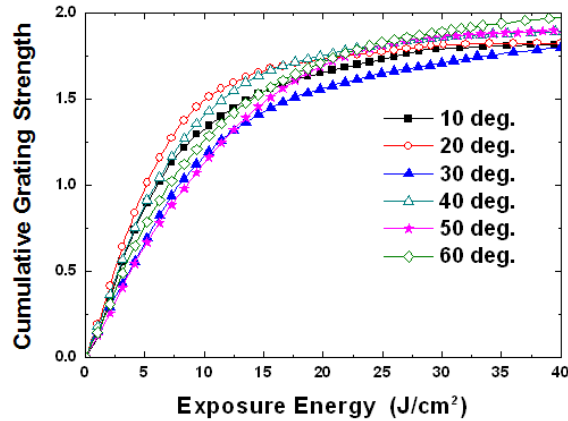


Fig. 4. The cumulative grating strengths for different writing angles under orthogonally circular polarization recording configuration.

Table 6. $M\#$ and S For Different Writing Angles of Orthogonal Circular Polarization Recording Configuration

Angle	$M\#$	$\Sigma (cm^2 \cdot J^{-1})$
10°	1.82	0.23
20°	1.83	0.29
30°	1.82	0.18
40°	1.90	0.24
50°	2.01	0.17
60°	2.01	0.19

4. Polarization multiplexing holographic memory using PQ/PMMA photopolymer

In this section we present an optical demonstration of polarization multiplexing holographic memory in PQ/PMMA photopolymer.

In order to combine polarization holograms with conventional multiplexing techniques, it is necessary to begin the design with holographic properties of the recording material. As was summarized in Table 5, polarization multiplexing with circular polarization configuration provides a better material performance of larger dynamic range and higher sensitivity. However, as was illustrated in Tables 2 & 4, the polarization state of the reconstructed signal will be always elliptically polarized and different from that of the object wave. Object waves of identical circular polarization can be reconstructed only when the polarization state of the reading beam is identical to that of the reference beam and at the same time paraxial approximation is satisfied.

In order to fulfill the paraxial approximation, we choose peristrophic multiplexing, because its selectivity is mainly constrained by the size of CCD, not intersection angle between the object and the reference beams, and so the angle can be arranged to be small. In experiments, the writing angle was set to be 10° to meet the paraxial approximation requirement. The sample was mounted on a rotation stage with the rotation axis parallel to the object beam. The schematic diagram for the optical setup is shown in Fig. 5. It is similar to the conventional holographic systems, except that three quarter-wave plates and a home-made liquid crystal phase retardation plate (LCPR) are added for the purpose of polarization control.

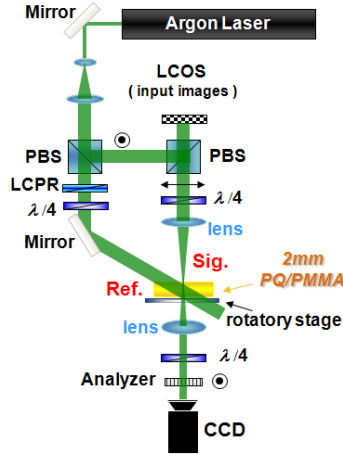


Fig. 5. Optical setup for circular polarization multiplexing holographic memory experiment.

For implementing polarization multiplexing, the polarization state of the object beam is fixed to be left-handed circularly polarized, and that of the reference beam can be switched between left-handed and right-handed circularly polarized by LCPR. At each position of the peristrophic multiplexing, two holograms are recorded one by one each with different circularly polarized reference beams. According to our definition, the hologram recorded with left-handed circularly polarized reference beam is an index hologram and the other recorded with right-handed circularly polarized reference beam is a polarization hologram.

During holograms recording stage, data pages were displayed on a liquid crystal on silicon (LCOS) spatial light modulator. The pair of two holograms was recorded at each position of the peristrophic multiplexing, then the rotation stage was rotated by 2° and next two data pages were recorded on the same area. In optical experiments, twenty pairs of holograms with objects of analog images have been recorded on one area of the medium.

During reconstruction stage, the holograms were reconstructed one by one with a reading beam of alternating polarizations. When the reading beam is left-handed circularly polarized, original object wave with left-handed circular polarization will be diffracted from the first hologram (the index hologram). The diffracted signal will pass through a quarter-wave plate to become s-polarized and finally transmits through the analyzer to reach CCD. On the other hand, according to the results illustrated in Table 2, this left-handed circularly polarized reading beam will not give any diffraction from the second hologram (the polarization hologram). The original object signal will be reconstructed correctly. However, if the paraxial approximation is violated, there would be a cross-talk noise from polarization hologram. The diffracted vector amplitude F_+ on CCD from the polarization hologram can be derived using case 2(a) in Table 2 and written as

$$F_+ \propto G_-^* F_+ G_+ \left[\frac{A+B_2}{2\sqrt{2}} \right] (1 - \cos^2(\theta_s - \theta_r)) \quad (15)$$

It can be seen that the diffracted signal increases with writing angle. Similarly, when the reading beam is switched to right-handed circularly polarized, the reconstructed signal from the first hologram (the index hologram) will be right-handed circularly polarized. It will become p-polarized after passing through the quarter-wave plate and so will be blocked by the analyzer. On the other hand, the diffracted signal reconstructed from the second hologram (the polarization hologram) will be left-handed polarized and thus can be imaged onto CCD. Therefore, each data page can be independently retrieved and imaged correctly onto CCD with the corresponding reading beam. The diffracted vector amplitude F_+ of cross-talk on CCD noise from index hologram under non-paraxial approximation can be written as

$$F_{+\infty} \frac{G_+ G_-^* F_-}{2\sqrt{2}} (1 - \cos(\theta_S - \theta_R))^2 \quad (16)$$

In experiments, the rotation stage is rotated to next angle and the next pair of holograms will be reconstructed, and so on. Figure 6 shows some of the reconstructed images. Among that, the left nine photos in Fig. 6(a) are reconstructed from the index holograms and the right nine photos in Fig. 6(b) are reconstructed from the polarization holograms. It can be seen that all the images are reconstructed correctly and the cross-talk noise is not significant.

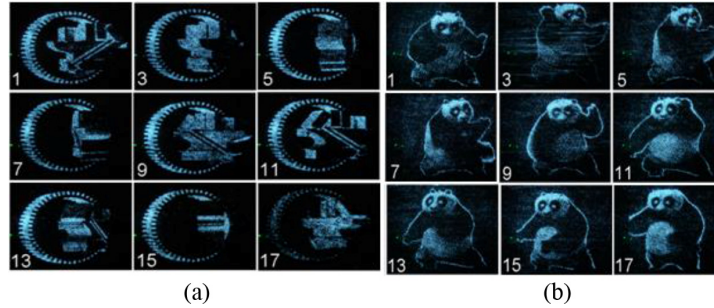


Fig. 6. Optical experimental results. (a). the left photos are reconstructed from the index holograms and (b). the right photos are reconstructed from the polarization holograms. The number on the corner indicates the order of recording.

5. Conclusions

Polarization holograms are recorded with writing beams of orthogonal polarizations in a polarization sensitive material. With the vectorial coupled wave theory, we have investigated the influence of the polarization states of the optical beams on the reconstructed signals from a polarization hologram. We have found that, in general, the polarization state of the reconstructed signal from a polarization hologram will not be the same as that of the original signal wave, unless all the optical waves are linearly polarized. For the orthogonal linear polarization holograms, original linearly polarized object wave can be reconstructed when the reading beam is identical to the reference beam. If the polarization of the reading beam is rotated by 90° , the polarization of the reconstructed signal will follow the rotation by 90° . For the orthogonal circular polarization holograms, under paraxial approximation, original object wave can be exactly reconstructed when the reading beam is identical to that of the reference beam. In this situation, there will be no diffraction if the polarization of the reading beam is orthogonally polarized with respect to the reference beam. Thus, circular polarization holograms provide a better distinction of the reading beams. We have performed experimental characterizations on holograms recording in 2-mm thick PQ/PMMA samples with orthogonal linearly and circularly polarized waves, respectively. It was found that the circularly polarized type possesses better dynamic range ($M\# = 1.82$) and material sensitivity ($S = 0.18 \text{ cm}^2 \cdot \text{J}^{-1}$), and the performance is comparable to that of the index hologram. Based on theoretical analyses and the material properties, a polarization multiplexing holographic memory using circularly polarized recording configuration has been designed and demonstrated. Twenty pairs of index and polarization holograms of analog images have been successfully recorded and reconstructed. The results show that holograms with reference beams of orthogonal polarizations recorded at the same area can be reconstructed independently by the reading beams with corresponding polarization states.

Acknowledgments

Financial support by National Science Council, Taiwan under contracts #NSC 101-2221-E-009-111-MY3 and #NSC 101-2221-E-009-112-MY3 are gratefully acknowledged.